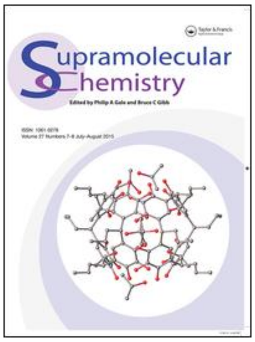

Supramolecular Chemistry

ISSN: 1061-0278 (Print) 1029-0478 (Online) Journal homepage: http://www.tandfonline.com/loi/gsch20

A highly selective fluorescent chemosensor for successive detection of Fe^{3+} and CN^- in pure water

Li Wang, Wen-Ting Li, Wen-Juan Qu, Jun-Xia Su, Qi Lin, Tai-Bao Wei & You-Ming Zhang

To cite this article: Li Wang, Wen-Ting Li, Wen-Juan Qu, Jun-Xia Su, Qi Lin, Tai-Bao Wei & You-Ming Zhang (2017): A highly selective fluorescent chemosensor for successive detection of Fe^{3+} and CN^- in pure water, Supramolecular Chemistry, DOI: 10.1080/10610278.2016.1277586

To link to this article: http://dx.doi.org/10.1080/10610278.2016.1277586

SUPRAMOLECULAR CHEMISTRY, 2017
http://dx.doi.org/10.1080/10610278.2016.1277586

Taylor & Francis
Taylor & Francis Group

A highly selective fluorescent chemosensor for successive detection of Fe^{3+} and CN^- in pure water

Li Wang, Wen-Ting Li, Wen-Juan Qu, Jun-Xia Su, Qi Lin, Tai-Bao Wei and You-Ming Zhang

Key Laboratory of Eco-Environment-Related Polymer Materials of Ministry of Education, Gansu Key Laboratory of Polymer Materials, College of Chemistry and Chemical Engineering, Northwest Normal University, Lanzhou, China

ABSTRACT

A water-soluble fluorescent chemosensor (**D**) based on 1, 8-naphthalimide derivative has been designed and synthesised as a new fluorescent sensor for successive detection of Fe^{3+} and CN^-. Fluorescence measurements show that chemosensor **D** has excellent fluorescent-specific selectivity and high sensitivity for Fe^{3+} over many other metal ions in pure water. Moreover, the complex of **D** and Fe^{3+} (**D–Fe^{3+}**) displayed high sensitivity for CN^- over many other anions in the same medium. Even more important, the recognition of the sensor **D** for Fe^{3+} and **D–Fe^{3+}** complex for CN^- could be used successfully in pure water. The test strips based on **D** and **D–Fe^{3+}** exhibited good selectivity to Fe^{3+} and CN,$^-$ respectively, we believe the test strips could serve as convenient and efficient Fe^{3+} and CN^- test kits.

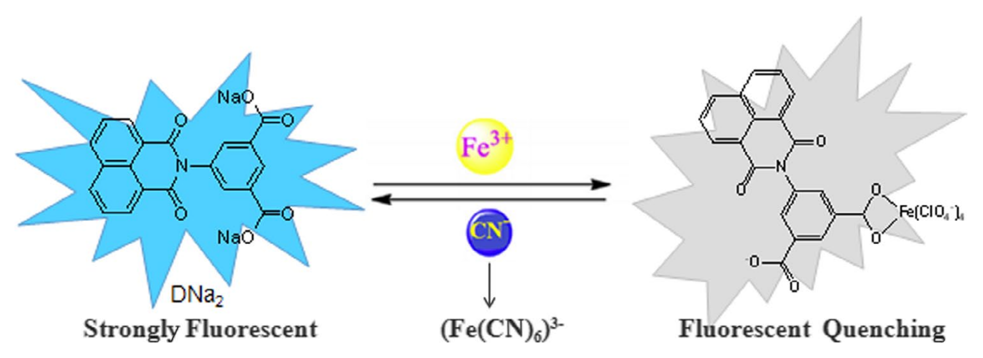

ARTICLE HISTORY
Received 22 July 2016
Accepted 23 December 2016

KEYWORDS
1, 8-naphthalimide; iron; cyanide; chemosensor; successive recognition; fluorescent

1. Introduction

In recent years, the design and synthesis of fluorescent chemosensors for cations and anions have been received extensive attention because of their fundamental role in medical, environmental and biological applications [*1–9*]. Bifunctional probes, which refer to those based on a single host that can independently recognise two guest species with distinct spectra responses by the same or different channels, have already emerged and have gradually become a new research focus in the field of fluorescence sensors [*10–16*].

Iron is the most abundant transition-metal ion in humans and other mammals, which plays important roles in various biological systems [*17–20*]. Moreover, excessive of iron ion is also harmful to the environment [*21*]. So the sensors for Fe^{3+} are badly needed [*22–26*]. Meanwhile, cyanide anion (CN^-) is extremely toxic to living organisms, and a trace amount of intake of the cyanide anion can therefore result in death [*27,28*]. The World Health Organisation (WHO) sets the maximum permissive level of cyanides in drinking water at 1.9 μM [*29*]. In addition, a large quantity of cyanide anion is widely used in industry for the synthesis of fine chemicals, electroplating and precious metal mining and so on [*30*]. Hence, the rational design and synthesis of efficient sensors to selectively detect CN^- at the environmental and biological levels have attracted much attention [*31–44*].

For practical applications of the probes in biochemical studies (especially for cell imaging studies), good water solubility is essential, because the usage of organic solvents usually destroys the normal function of biomolecules [*45*]. Although previous work has involved the development

CONTACT You-Ming Zhang ✉ zhangnwnu@126.com; Tai-Bao Wei ✉ weitaibao@126.com

Supplemental data for this article can be accessed at http://dx.doi.org/10.1080/10610278.2016.1277586.

of a wide variety of chemical and physical sensors for the detection of CN^-, so far, improving the detection selectivity and sensitivity in the context of interference from coexisting anions such as F^- and AcO^- in pure water has been challenging.

In view of these and base on our research interesting in ions recognition [*46–58*], we want to develop a water-soluble sensor. In this paper, a water soluble chemosensor (**D**) based on 1, 8-naphthalimide derivative has been designed and synthesised as a new fluorescent sensor for successive detection of Fe^{3+} and CN^-. The strategy for the design of the chemosensor (**D**) was as follow. The 1, 8-naphthalimide group acts as fluorophore [*59–64*], carboxyl group acts as coordinate group and hydrophilic group. We are very gratifying to see that the results go as we expect, sensor **D** displays high sensitivity and rapid response (<1 min) for recognising Fe^{3+} in pure aqueous system. Excitingly, **D–Fe**$^{3+}$ displays high sensitivity for cyanide in same system, successfully achieve successive detection of Fe^{3+} and CN^-.

2. Experimental section

2.1. Materials and apparatus

Fresh double-distilled water was used throughout the experiment. All other reagents and solvents were commercially available at analytical grade and were used without further purification. ^1H NMR spectra was recorded on an Agilent DD2 at 600 MHz spectra. ^1H chemical shifts are reported in ppm downfield from tetramethylsilane (TMS, δ scale with the solvent resonances as internal standards). UV–visible spectra were recorded on a Shimadzu UV–2550 spectrometer. Fluorescence spectra were recorded on a Shimadzu RF–5310. Melting points were measured on an X–4 digital melting-point apparatus. The infrared spectra were performed on a Digilab FTS–3000 FT–IR spectrophotometer. Mass spectra were performed on a Bruker Esquire 3000 plus mass spectrometer (Bruker–FranzenAnalytik GmbH Bremen, Germany) equipped with ESI interface and ion trap analyser.

2.2. Synthesis of the chemosensor D

Compound **D** can be readily prepared by a simple and low-cost acetylation reaction of 5-aminoisophthalic acid group and 1, 8-naphthalic anhydride (Scheme 1). 5-aminoisophthalic acid (0.72 g, 4.0 mmol) and 1, 8-naphthalic anhydride (0.79 g, 4.0 mmol) were combined in hot absolute DMF (20 mL). The solution was stirred under reflux conditions for 8 h, after cooling to room temperature, the white precipitate was filtrated, washed with absolute ethanol three times and dried under vacuum, then get the product **D** in 77% yield (m.p. > 300 °C). The chemosensor **D** has been characterised by ^1H NMR and IR, ^1H NMR (DMSO-d_6, 600 MHz): δ 13.46 (s 2H), δ 8.51–8.56 (m 5H), δ 8.25 (s 2H), 7.90–7.92 (t 2H). IR (KBr, cm^{-1}) ν: 3349 (w), 1699 (s), 1585 (m), 1411 (w), 1348 (w), 1282 (w), 923 (w) (Figure S1 and S2). **D** has two terminal carboxylic acid groups, and because of the strong intermolecular H–bonding interaction in the solid state, the solubility of **D** is very poor in water. To alleviate the problem of solubility in water, we have dissolved it by adding two equivalents of NaOH that converts –COOH groups to sodium salt of **D**, and because of the ionic character of the latter, **D** after deprotonation could be completely dissolved in pure water media. Mass spectrometry was made with sodium salt of **D** (D^{2-}) (Figure S3). ESI–MS *m/z*: calcd for $C_{20}H_{10}NO_6$, $[D^{2-}+H] = 360.0508$, found $[D^{2-}+H] = 360.0550$.

2.3. General procedure for UV–vis experiments

All UV–vis spectra were recorded on a Shimadzu UV–2550 spectrometer after the addition of perchlorate metal salts and sodium salt of anion in water, while keeping the ligand concentration constant (2.0×10^{-5} M).

2.4. General procedure for fluorescence spectra experiments

All fluorescence spectra were recorded on a Shimadzu RF–5301 fluorescence spectrometer after the addition of perchlorate metal salts and sodium salt of anion in water, while keeping the ligand concentration constant (2.0×10^{-5} M). The excitation wavelength was 310 nm.

3. Results and discussion

In order to investigate the Fe^{3+} recognition abilities of the sensor **D**, we carried out a series of Host–Guest recognition

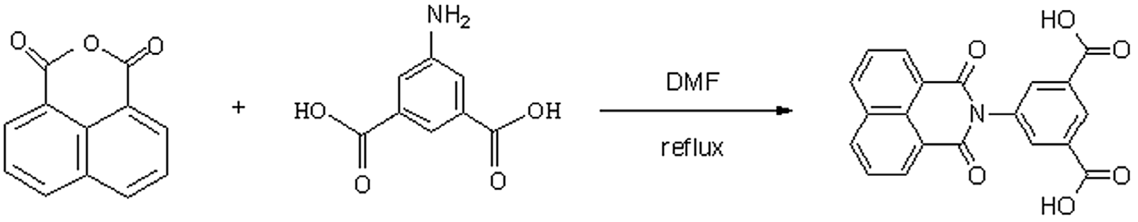

Scheme 1. Synthetic procedures for sensor D.

experiments in pure water. The recognition profiles of the chemosensor **D** towards various metal ions that include Fe^{3+}, Ag^{+}, Ca^{2+}, Cu^{2+}, Co^{2+}, Ni^{2+}, Cd^{2+}, Zn^{2+} and Mg^{2+} were primarily investigated by UV-vis spectroscopy (Figure S4) and fluorescence spectroscopy in water. Upon adding 20 equivalents of Fe^{3+} to the water solution of sensor **D**, the absorption at 348 nm enhanced immediately, and a broad shoulder peak appeared in a region from 350 to 420 nm, the same tests were also conducted using Ag^{+}, Ca^{2+}, Cu^{2+}, Co^{2+}, Ni^{2+}, Cd^{2+}, Zn^{2+} and Mg^{2+} ions, and none of these cations induced any significant changes, while 20 equivalents of Cu^{2+} to the water solution of sensor **D**, the absorption at 348 nm weakened slightly, and a weak broad shoulder peak from 375 to 500 nm is observed, but it did not interfere with the recognition of the sensor **D** to Fe^{3+} (Figure S4). As shown in Figure 1, in the fluorescence spectrum, the maximum emission of **D** appeared at 396 nm in water when excited at $\lambda_{ex} = 310$ nm. When 20 equivalents of Fe^{3+} was added to the water solution of sensor **D**, the fluorescence emission peak at 396 nm disappeared. The drastic color change from blue to colourless could be distinguished by naked-eyes through UV lamp. To further explore the selectivity of sensor **D**, the same tests were also conducted using Ag^{+}, Ca^{2+}, Cu^{2+}, Co^{2+}, Ni^{2+}, Cd^{2+}, Zn^{2+} and Mg^{2+} ions, and no significant changes were observed in the fluorescent spectrum of the sensor **D** (Figure 2). Therefore, in pure water solution, **D** showed specific fluorescent selectivity to Fe^{3+}.

In order to investigate the CN^{-} recognition abilities of the sensor **D–Fe³⁺**, a series of Host-Guest recognition experiments in pure water were also carried out. The recognition profiles of the chemosensor **D–Fe³⁺** complex towards various anions were primarily investigated by UV–vis spectroscopy (Figure S5) and fluorescence spectroscopy in water. It can be seen that the shape of the absorption curve of **D + Fe³⁺+CN⁻** is consistent with **D**, while the shape of the absorption curve which the other anions that we studied, such as F^{-}, Cl^{-}, Br^{-}, I^{-}, AcO^{-}, ClO_4^{-} and SCN^{-} remain basically the same with **D–Fe³⁺**, showed the selectivity of sensor **D–Fe³⁺** to CN^{-} in pure water solution (Figure S5). As shown in Figure 3, the completely quenched fluorescence of **D** in water by Fe^{3+} was turned on after the addition of CN^{-}. To evaluate the selectivity of **D–Fe³⁺** complex towards CN^{-}, the influence of other anions, such as F^{-}, Cl^{-}, Br^{-}, I^{-}, AcO^{-}, ClO_4^{-} and SCN^{-}, was investigated. However, the competitive anions did not produce any substantial effect on emission spectra. These results suggested that sensor **D** displayed high selectivity towards Fe^{3+} in pure water, and the resulting **D–Fe³⁺** complex system displayed an excellent selectivity for CN^{-} in the same media as well (Figure 4). To this end, the designed successive recognition of the two ions has been achieved with relay specificity ($Fe^{3+} \rightarrow CN^{-}$) via a fluorescence 'on–off–on' switching mechanism and provided a complementary sensing approach to previous bifunctional probes for Fe^{3+} and CN^{-} ions.

To further investigate the sensing properties of **D** and **D–Fe³⁺**, fluorescence titration experiments were performed. Figure 5 shows that with the addition of increasing amounts of Fe^{3+} to the water solution of sensor **D**, the fluorescence emission intensity of **D** at λ max = 396 nm was decreased gradually, and the fluorescence of **D** was essentially quenched by 6.12 equiv of Fe^{3+} ion. The binding

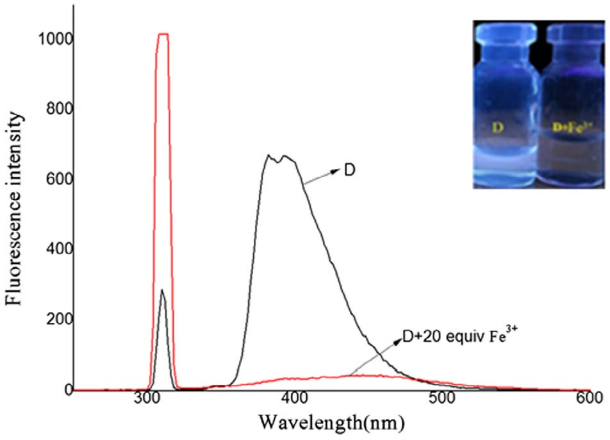

Figure 1. (Colour online) Fluorescence spectra of **D** (20 μM) upon an excitation at 310 nm in pure water media in the presence of Fe^{3+} (20 equiv.). Inset: photographfrom left to right shows the change in the fluorescence of **D**, **D–Fe³⁺** (20equiv.) in pure water.

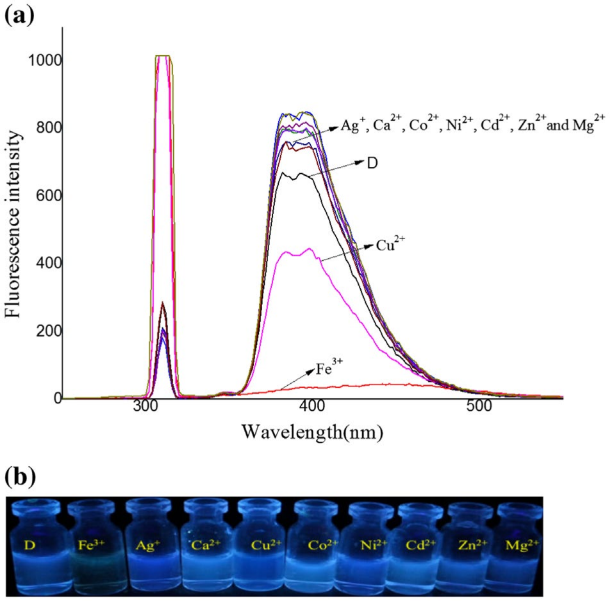

Figure 2. (Colour online) (a) Fluorescence emission data for 1:20 mixture of D (20 μM) and different metal ions, as their perchlorate salts in pure water . (λ_{ex} = 310 nm). (b) Visual fluorescence emissions of sensor D after the addition of Fe^{3+}, Ag^{+}, Ca^{2+}, Cu^{2+}, Co^{2+}, Ni^{2+}, Cd^{2+}, Zn^{2+} and Mg^{2+} (20 equiv.) in pure water media on excitation at 310 nm using UV lamp at room temperature.

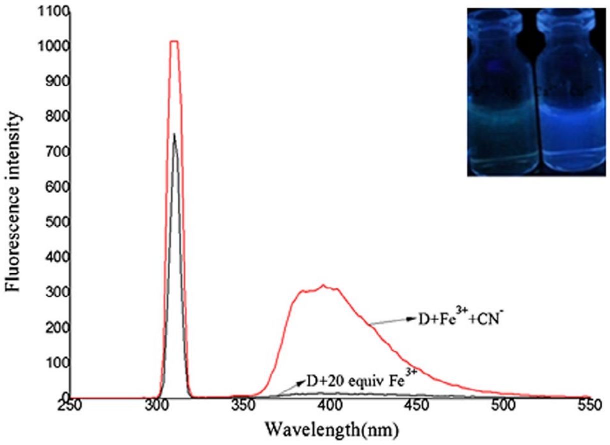

Figure 3. (Colour online) Fluorescence spectra of **D–Fe^{3+}** (20 μM) upon an excitation at 310 nm in pure water media in the presence of CN$^-$(50 equiv.). Inset: photograph from left to right shows the change in the fluorescence of **D–Fe^{3+}**, D + Fe^{3+}+CN$^-$ (50 equiv.) in pure water.

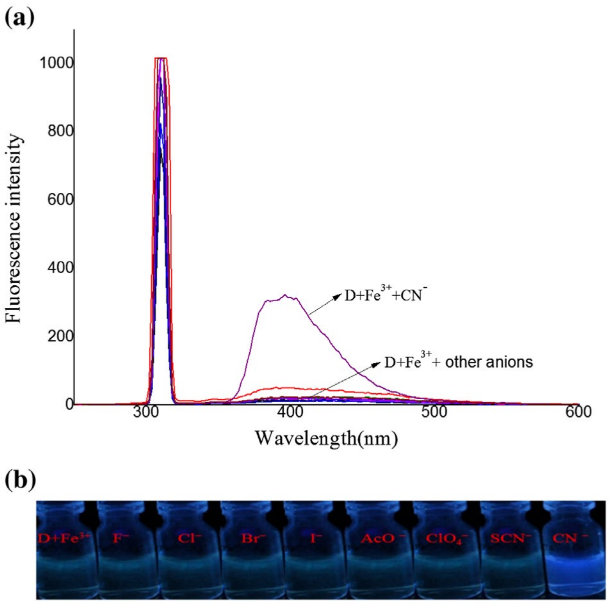

Figure 4. (Colour online) (a) Fluorescence emission data for **D–Fe^{3+}** (20 μM) and different anions (50 equiv.) as their sodium salts in pure water. (excitation wavelength = 310 nm). (b) Visual fluorescence emissions of sensor **D–Fe^{3+}** (20 μM) after the addition of F$^-$, Cl$^-$, Br$^-$, I$^-$, AcO$^-$, ClO$_4^-$, CN$^-$, SCN$^-$ (50 equiv.) in water on excitation at 365 nm using UV lamp at room temperature.

constant Ka of the metal complex was determined as 4.57 × 10^4 M^{-1}, obtained by a linear curve fitting of the fluorescence titration results (Supporting Information). And the detection limit of the **D** for the determination of Fe^{3+} was estimated to be 1.97 × 10^{-7} M (Figure S6), which point to the high detection sensitivity. The generated **D–Fe^{3+}** was directly used to titrating CN$^-$ without separation and purification. Upon the addition of CN$^-$, there is a significant increase in the fluorescence intensity of **D–Fe^{3+}** (Figure 6). And the detection limit of the **D–Fe^{3+}** for the determination of CN$^-$ was estimated to be 2.6 × 10^{-10} M (Figure S7). Obviously, the detection limit of the sensor **D–Fe^{3+}** is lower than the WHO limit(1.9 μM).

The selectivity towards Fe^{3+} and CN$^-$ were further ascertained by the competition experiments. Figure 7 illustrated clearly the fluorescence response of **D** to Fe^{3+} in the presence of other metal ions. From the bar diagram, we could easily understand that all the coexistent metal ions had no obvious interference with the detection of Fe^{3+}. In the presence of these coexistent cations, the Fe^{3+} still produced similar fluorescence emission changes. The result suggested that sensor **D** could serve as a fluorescent chemosensor for Fe^{3+} in water solution. Likewise, Figure 8

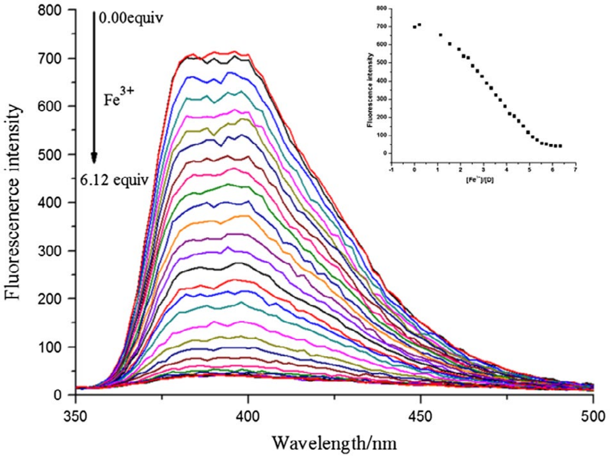

Figure 5. (Colour online) Fluorescence spectra of **D** (20 μM) in pure water in the presence of increasing amounts of Fe(ClO$_4$)$_3$. Inset: A plot of fluorescence intensity depending on the concentration of Fe^{3+} in the range from 0 to 6.12 equiv. The excitation wavelength was 310 nm.

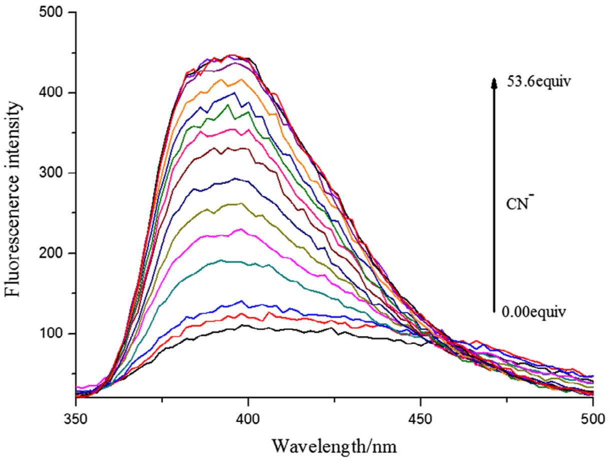

Figure 6. (Colour online) Fluorescence spectra of **D–Fe^{3+}** (20 μM) in pure water in the presence of increasing amounts of CN$^-$. The excitation wavelength was 310 nm.

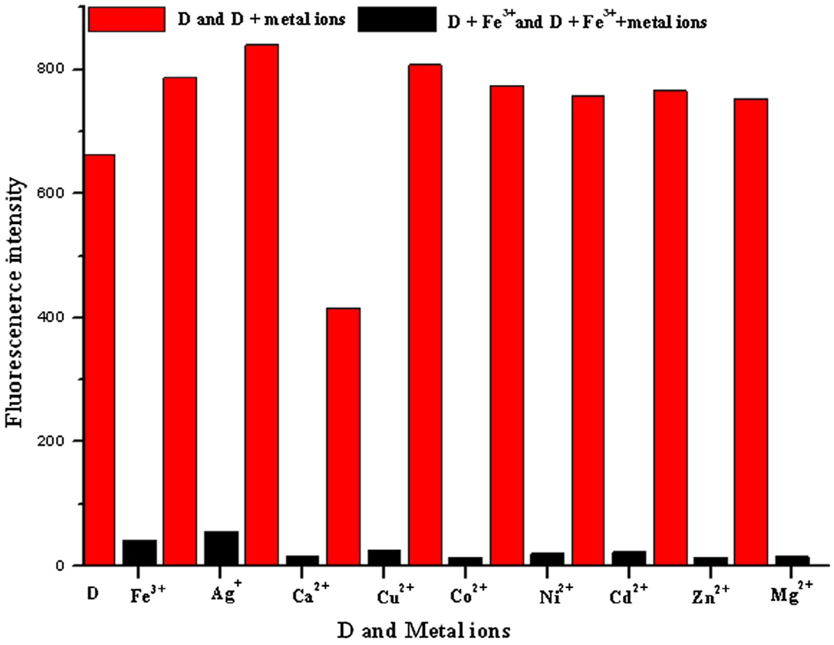

Figure 7. (Colour online) Competitive experiments towards the fluorescence quenching effect of Fe^{3+} in presence of a large number of other cations (20 equiv.).

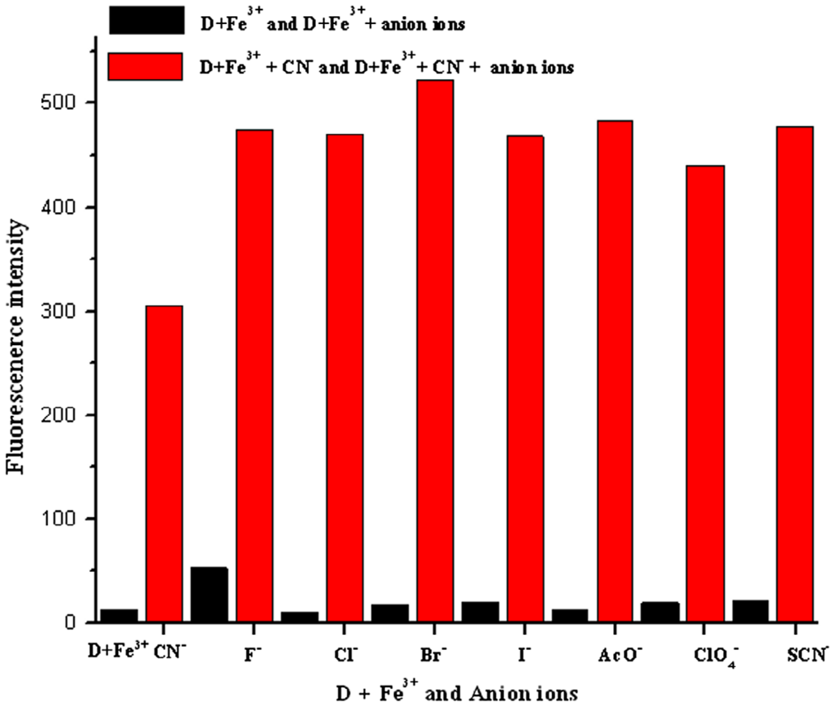

Figure 8. (Colour online) Normalised change in the emission intensity of **D–Fe**$^{3+}$ after addition of the CN^- (50 equiv.) in the presence of an excess amount of other anions (50 equiv.).

indicated that the selectivity of **D–Fe**$^{3+}$ towards CN^- is hardly affected by these commonly coexistent ions.

Besides the fluorescence change, infrared (IR) spectrum of the ferric complex is compared to the metal-free ligand spectrum in Figure S2. The dominant C=O stretching vibration is seen at 1701 cm^{-1} (red line in Figure S2). In contrast, the typical C=O vibration in the **D–Fe**$^{3+}$ spectrum at 1699 cm^{-1} and broadens which accounts for coordination of the carbonyl oxygen to Fe^{3+} (black line in Figure S2). The shift to low wavenumbers and broadening of these absorption bands suggested the coordination of Fe^{3+} with the carbonyl groups of **D** induced the formation of the ferric complex.

In order to further quantify the complexation ratio between D and Fe^{3+}, the Job's method was used (Figure 9). As shown in Figure 9, Job's plot of D and Fe^{3+}, we can see there is an inflection point when the molar fraction of $[D]/([D]+[Fe^{3+}])$ was 0.5, the result showing the formation of a 1:1 bonding mode between **D** and Fe^{3+}. From the ESI–MS spectrum, we can also see an obvious peak at *m/z* 360.0550 assignable to $[D^{2-} + H]$ (Figure S3) and a peak at m/z 851.1862 assignable to $[D^{2-} + Fe^{3+} + 4ClO_4^- + K^+ + H^+]$ (Figure S8). The presence of Fe^{3+} leads to the formation of **D–Fe³⁺**, which is then converted to a structural change, sensor **D** is most likely to chelate with metal ions via its carbonyl O adopting the more familiar Fe–O–C–O–Fe modes [65]. Meanwhile, Fe^{3+} is coordinates with ClO_4^- (Scheme 2).We have also prepared **D–Fe³⁺** complex solid, from the ESI–MS spectrum (Figure S9), the ion peaks were detected at m/z 437.09, which correspond to $[D^{2-} + Fe^{3+} + Na^+]$, the result proved the 1:1 bonding mode between **D** and Fe^{3+} again.

To investigate the practical application of chemosensor **D**, test strips were prepared by immersing filter papers into a water solution of D (2.0×10^{-4} mol/L) and then drying in air. The test strips containing D were utilised to sense Fe^{3+} first. When Fe^{3+} was added on the test kits, the fluorescence turn off response can be observed under UV irradiation. The same procedures were done for cyanide and competitive ions (Figure 10). The fluorescence turn on response can also be seen under UV irradiation. However, potentially competitive ions exerted no influence on the detection of iron and cyanide by the test strips. Therefore, the test strips could conveniently detect iron and cyanide in water solution.

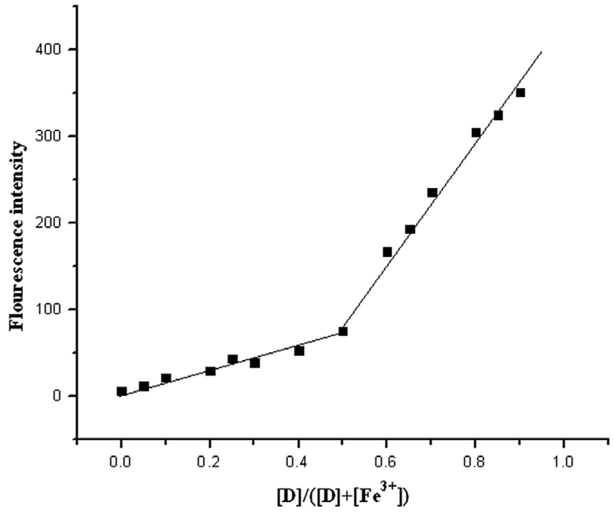

Figure 9. Job's plot of D and Fe^{3+}, which indicated the stoichiometry of **D–Fe³⁺** complex is 1:1.

Figure 10. (Colour online) Photographs of the colorimetric test kits with D (**D–Fe³⁺**) for detecting Fe^{3+} (CN^-) using UV lamp at rt.

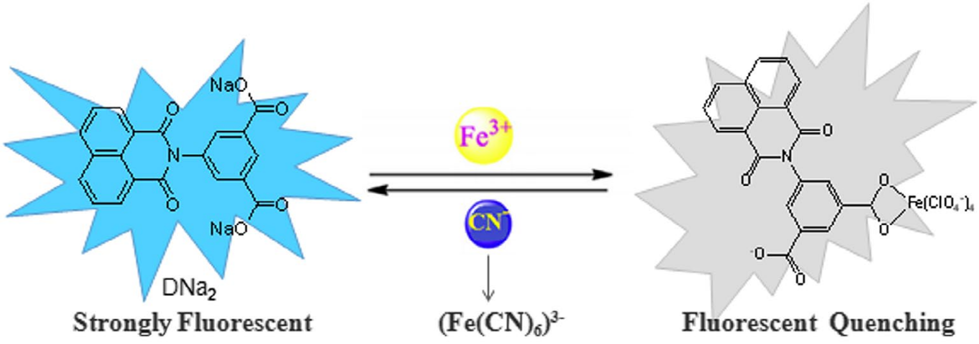

Scheme 2. (Colour online) Possible binding mode of sensor **D** with Fe^{3+}.

4. Conclusions

In summary, we have developed a water-soluble fluorescent chemosensor (**D**) based on 1, 8-naphthalimide derivative for the successive recognition of two ions (Fe^{3+} and CN^{-}). The sensor **D** displayed high selectivity and sensitivity for Fe^{3+} in water solution, which served as an on-off-type sensor. Consequently, the **D–Fe^{3+}** complex showed highly selective and sensitive response towards CN^{-} in the same media, constituting an on–off–on-type fluorescence recognition system. The detection limits of the sensor **D** to Fe^{3+} is 1.97×10^{-7} M and the **D–Fe^{3+}** complex to CN^{-} anion is 2.6×10^{-10} M respectively. Moreover, the sensors **D** and the **D–Fe^{3+}** complex could be used in pure water system, which is very important for good sensor. Test strips based on **D** and **D–Fe^{3+}** were prepared, which could conveniently and efficiently detect Fe^{3+} and CN^{-}.

Disclosure statement

No potential conflict of interest was reported by the authors.

Funding

This work was supported by the National Natural Science Foundation of China (NSFC) [Number 21662031], [Number 21661028], [Number 21574104], [Number 21262032]; The Program for Changjiang Scholars and Innovative Research Team in University of Ministry of Education of China [IRT 15R56].

References

(1) Cort, A.D.; Forte, G.; Schiaffino, L. *J. Org. Chem.* **2011**, *76*, 7569–7572.

(2) Li, Y.P.; Yang, H.R.; Zhao, Q.; Song, W.C.; Han, J.; Bu, X.H. *Inorg. Chem.* **2012**, *51*, 9642–9648.

(3) Zhang, Y.M.; Lin, Q.; Wei, T.B.; Wang, D.D.; Yao, H.; Wang, Y.L. *Sens. Actuators B* **2009**, *137*, 447–455.

(4) Hu, J.H.; Yan, N.P.; Chen, J.J. *J. Chem. Res.* **2012**, *36*, 619–622.

(5) Yang, Y.L.; Wang, Y.W.; Peng, Y. *Sci. China Chem.* **2014**, *57*, 289–295.

(6) Hu, J.H.; Li, J.B.; Qi, J.; Chen, J.J. *New J. Chem.* **2015**, *39*, 843–848.

(7) Dong, W.K.; Akogun, S.F.; Zhang, Y.; Sun, Y.X.; Dong, X.Y. *Sens. Actuators B* **2017**, *238*, 723–734.

(8) Hu, J.H.; Li, J.B.; Qi, J.; Sun, Y. *Sens. Actuators B* **2015**, *208*, 581–587.

(9) Hu, J.H.; Li, J.B.; Qi, J.; Sun, Y. *Sulfur Silicon* **2016**, *191*, 984–987.

(10) Zhu, Y.R.; Li, H.; Yan, G.T.; Shi, B.B.; Zhang, Y.M.; Lin, Q.; Yao, H.; Wei, T.B. *RSC Adv.* **2015**, *5*, 49953–49957.

(11) Ravikumar, I.; Ghosh, P. *Inorg. Chem.* **2011**, *50*, 4229–4231.

(12) Liu, J.; Lin, Q.; Zhang, Y.M.; Wei, T.B. *Sci. China Chem.* **2014**, *57*, 1257–1263.

(13) Dong, Y.M.; Peng, Y.; Dong, M.; Wang, Y.W. *J. Org. Chem.* **2011**, *76*, 6962–6966.

(14) Kumari, N.; Jha, S.; Bhattacharya, S. *J. Org. Chem.* **2011**, *76*, 8215–8222.

(15) Liu, J.; Xie, Y.Q.; Lin, Q.; Shi, B.B.; Zhang, P.; Zhang, Y.M.; Wei, T.B. *Sens. Actuators B* **2013**, *186*, 657–665.

(16) Dong, W.K.; Li, X.L.; Wang, L.; Zhang, Y.; Ding, Y.J. *Sens. Actuators B* **2016**, *229*, 370–378.

(17) Sahoo, S.K.; Sharma, D.; Bera, R.K.; Crisponi, G. *Chem. Soc. Rev.* **2012**, *41*, 7195–7179.

(18) Kumar, M.; Kumar, R.; Bhalla, V. *Org Lett.* **2011**, *13*, 366–369.

(19) Xu, M.Y.; Wu, S.Z.; Zeng, F.; Yu, C.M. *Langmuir* **2010**, *26*, 4529–4534.

(20) Chen, Y.C.; Liu, X.X.; Huang, H.; Wu, W.W.; Zheng, Y.S. *Sci. China Chem.* **2010**, *53*, 569–575.

(21) Li, Z.X.; Zhang, L.F.; Li, X.Y.; Guo, Y.K.; Ni, Z.H.; Chen, J.H.; Wei, L.H.; Yu, M.M. *Dyes Pigm.* **2012**, *94*, 60–65.

(22) Zhao, L.L.; Xin, X.; Ding, P.; Song, A.X.; Xie, Z.C.; Shen, J.L.; Xu, G.Y. *Anal. Chim. Acta* **2016**, *926*, 99–106.

(23) Xie, J.Y.; Li, C.Y.; Li, Y.F.; Fu, Y.J.; Nie, S.X.; Tan, H.-Y. *Dyes Pigm.* **2017**, *136*, 817–824.

(24) He, Y.H.; Lai, J.P.; Sun, H.; Chen, Z.M.; Lan, S. *Sens. Actuators B: Chem.* **2016**, *225*, 405–412.

(25) Liu, W.; Diao, H.P.; Chang, H.H.; Wang, H.J.; Li, T.T.; Wei, W.L. *Sens. Actuators B: Chem.* **2017**, *241*, 190–198.

(26) Gao, Y.; Liu, H.M.; Liu, Q.L.; Wang, W. *Tetrahedron Lett.* **2016**, *57*, 1852–1855.

(27) Wu, W.L.; Xiao, Q.W.; Zhang, P.; Ye, M.; Wan, Y.P.; Liang, H.X. *Food Chem.* **2015**, *172*, 681–684.

(28) Xu, Y.; Dai, X.; Zhao, B.X. *Spectrochim. Acta, Part A* **2015**, *138*, 164–168.

(29) Rozov, I. *New WHO Guidelines for Drinking-water Quality, Clin Pharm;* World Health Organization: Geneva. 1996.

(30) Young, C.; Tidwell, L.; Anderson, C. *Cyanide: Social, Industrial, and Economic Aspects, Minerals*; Metals & Materials Society: Warrendale, 2001.

(31) Hu, J.H.; Sun, Y.; Qi, J.; Pei, P.X.; Lin, Q.; Zhang, Y.M. *RSC Adv.* **2016**, *6*, 100401–100406.

(32) Du, J.J.; Hu, M.M.; Fan, J.L.; Peng, X.J. *Chem. Soc. Rev.* **2012**, *41*, 4511–4535.

(33) Hu, J.H.; Yan, N.P.; Chen, J.J.; Li, J.B. *Chem. J. Chinese U.* **2013**, *34*, 1368–1373.

(34) Yang, Y.M.; Zhao, Q.; Feng, W.; Li, F.Y. *Chem. Rev.* **2013**, *113*, 192–270.

(35) Hu, J.H.; Chen, J.J.; Li, J.B.; Qi, J. *Chin. J. Inorg. Chem.* **2014**, *30*, 2544–2548.

(36) Zhang, P.; Shi, B.B.; You, X.M.; Zhang, Y.M.; Lin, Q.; Yao, H.; Wei, T.B *Tetrahedron* **2014**, *70*, 1889–1894.

(37) Li, J.B.; Hu, J.H.; Chen, J.J.; Qi, J. *Spectrochimica. Acta Part A* **2014**, *133*, 773–777.

(38) Zhu, X.; Lin, Q.; Lou, J.C.; Lu, T.T.; Zhang, Y.M.; Wei, T.B. *New J. Chem.* **2015**, *39*, 7206–7210.

(39) Hu, J.H.; Li, J.B.; Qi, J.; Sun, Y. *New J. Chem.* **2015**, *39*, 4041–4046.

(40) Li, Q.; Zhang, J.H.; Cai, Y.; Qu, W.J.; Gao, G.Y.; Lin, Q.; Yao, H.; Zhang, Y.M.; Wei, T.B. *Tetrahedron* **2015**, *71*, 857–862.

(41) Sun, Y.; Hu, J.H.; Qi, J.; Li, J.B. *Spectrochimica. Acta Part A* **2016**, *167*, 101–105.

(42) Wei, T.B.; Li, W.T.; Li, Q.; Su, J.X.; Qu, W.J.; Lin, Q.; Yao, H.; Zhang, Y.M. *Tetrahedron Lett.* **2016**, *57*, 2767–2771.

(43) Zhang, W.; Xu, K.X.; Yue, L.X.; Shao, Z.L.; Feng, Y.; Fang, M. *Dyes Pigm.*, **2017**, *137*, 560–568.

(44) Wang, L.Y.; Li, L.Q.; Cao, D.R. *Sens. Actuators B: Chem.* **2017**, *239*, 1307–1317.

(45) Li, X.H.; Gao, X.H.; Shi, W.; Ma, H.M. *Chem. Rev.* **2014**, *114*, 590–659.

(46) Qu, W.J.; Gao, G.Y.; Shi, B.B.; Zhang, P.; Wei, T.B.; Lin, Q.; Yao, H.; Zhang, Y.M. *Supra. Chem.* **2014**, *26*, 403–408.

(47) Lin, Q.; Sun, B.; Yang, Q.P.; Fu, Y.P.; Zhu, X.; Zhang, Y.M.; Wei, T.B. *Chem. Commun.* **2014**, *50*, 10669–10671.

(48) Lin, Q.; Sun , B.; Yang , Q.P.; Fu, Y.P.; Zhu, X.; Wei, T.B.; Zhang, Y.M. *Chem. Eur. J.* **2014**, *20*, 11457–11462.

(49) Lin, Q.; Lu, T.T.; Zhu, X.; Sun, B.; Yang, Q.P.; Wei, T.B.; Zhang, Y.M. *Chem. Commun.* **2015**, *51*, 1635–1638.

(50) Zhang, Y.M.; You, X.M.; Yao, H.; Guo, Y.; Zhang, P.; Shi, B.B.; Liu, J.; Lin, Q.; Wei, T.B. *Supra. Chem.* **2014**, *26*, 39–47.

(51) Wu, G.Y.; Hu, B.; Shi, B.B.; Zhang, P.; Lin, Q.; Yao, H.; Zhang, Y.M.; Wei, T.B. *Supra. Chem.* **2015**, *27*, 201–211.

(52) Yan, G.T.; Li, H.; Zhu, Y.R.; Shi, B.B.; Qu, W.J.; Lin, Q.; Yao, H.; Zhang, Y.M.; Wei, T.B. *New J. Chem.* **2015**, *39*, 8797–8801.

(53) Li, H.; Zhu, Y.R.; Shi, B.B.; Qu, W.J.; Zhang, Y.M.; Lin, Q.; Yao, H.; Wei, T.B. *Supra. Chem.* **2015**, *27*, 471–477.

(54) Cheng, X.; Li, H.; Zheng, F.; Lin, Q.; Zhang, Y.M.; Yao, H.; Wei, T.B. *Dyes Pigm.* **2016**, *127*, 59–66.

(55) Lin, Q.; Yang, Q.P.; Sun, B.; Lou, J.C.; Wei, T.B.; Zhang, Y.M. *RSC Adv.* **2015**, *5*, 11786–11790.

(56) Wei, T.B.; Li, H.; Zhu, Y.R.; Lu, T.T.; Shi, B.B.; Lin, Q.; Yao, H.; Zhang, Y.M. *RSC Adv.* **2015**, *5*, 60273–60278.

(57) Lin, Q.; Zhu, X.; Fu, Y.; Yang, Q.; Sun, B.; Wei, T.B.; Zhang, Y.M. *Dyes Pigm.* **2015**, *113*, 748–753.

(58) Gao, G.Y.; Qu, W.J.; Shi, B.B.; Lin, Q.; Yao, H.; Zhang, Y.M.; Chang, J.; Cai, Y.; Wei, T.B. *Sens. Actuators B: Chem.* **2015**, *213*, 501–507.

(59) de Silva, A.P.; Moody, T.S.; Wright, G.D. *Analyst.* **2009**, *134*, 2385–2393.

(60) Duke, R.M.; Veale, E.B.; Pfeffer, F.M.; Kruger, P.E.; Gunnlaugsson, T. *Chem. Soc. Rev.* **2010**, *39*, 3936–3953.

(61) Zheng, S.P.L.; Lynch, P.L.M.; Rice, T.E.; Moody, T.S.; Gunaratne, H.Q.N.; de Silva, A.P. *Photochem. Photobiol. Sci.* **2012**, *11*, 1675–1681.

(62) Banerjee, S.; Veale, E.B.; Phelan, C.M.; Murphy, S.A.; Tocci, G.M.; Gillespie, L.J.; Frimannsson, D.O.; Kelly, J.M.; Gunnlaugsson, T. *Chem. Soc. Rev.* **2013**, *42*, 1601–1608.

(63) Wu, H.L.; Wang, C.P.; Zhang, Y.H.; Chen, C.Y.; Yang, Z.H.; Fan, X.Y. Z. Naturforsch. **2015**, *70*, b: 863–869.

(64) Reger, D.L.; Leitner, A.P.; Smith, M.D. *Cryst. Growth Des.* **2016**, *16*, 527–536.

(65) (a) Dong, W.K.; Sun, Y.X.; Zhao, C.Y.; Dong, X.Y.; Xu, L. *Polyhedron* **2010**, *29*, 2087–2097; (b) Wang, P.; Zhao, L. *Spectrochim. Acta, Part A* **2015**, *135*, 342–350; (c) Sun, Y.X.; Dong, W.K.; Wang, L.; Zhao, L.; Yang, Y.H. *Chin. J. Inorg. Chem.* **2009**, *25*, 1478–1482; (d) Dong, W.K.; Ma, J.C.; Zhu, L.C.; Zhang, Y.; Li, X.L. *Inorg. Chim. Acta* **2016**, *445*, 140–148; (e) Dong, W.K.; Lan, P.F.; Zhu, W.M.; Zhang, Y. *J. Coord. Chem.* **2016**, *69*, 1272–1283; (f) Dong, W.K.; Zhang, F.; Li, N.; Xu, L.; Zhang, Y.; Zhang, J.; Zhu, L.C. *Z. Anorg. Allg. Chem.* **2016**, *642*, 532–538; (g) Dong, X.Y.; Sun, Y.X.; Wang, L.; Li, L. *J. Chem. Res.* **2012**, 387–390; (h) Yu, T.Z.; Zhang, K.; Zhao, Y.L.; Yang, C.H.; Zhang, H.; Fan, D.W.; Dong, W.K. *Inorg. Chem. Commun.* **2007**, *10*, 401–403; (i) Yu, T.Z.; Zhang, K.; Zhao, Y.L.; Yang, C.H.; Zhang, H.; Qian, L.; Fan, D.W.; Dong, W.K.; Chen, L.L.; Qiu, Y.Q. *Inorg. Chim. Acta* **2008**, *361*, 233–240; (j) Dong, W.K.; Ma, J.C.; Zhu, L.C.; Zhang, Y. *New J. Chem* **2016**, *40*, 6998–7010; (k) Dong, W.K.; Zhang, J.; Zhang, Y.; Li, N. *Inorg. Chim. Acta* **2016**, *444*, 95–102; (l) Dong, W.K.; Duan, J.G.; Guan, Y.H.; Shi, J.Y.; Zhao, C.Y. *Inorg. Chim. Acta* **2009**, *362*, 1129–1134; (m) Dong, W.K.; Ma, J.C.; Zhu, L.C.; Sun, Y.X.; Akogun, S.F.; Zhang, Y. *Cryst. Growth Des.* **2016**, *16*, 6903–6914.